Newtonian limit of scalar-tensor theories and galactic dynamics: isolated and interacting galaxies

J.L. Cervantes-Cota*, M.A. Rodríguez-Meza, R. Gabbasov, and J. Klapp
Depto. de Física, Instituto Nacional de Investigaciones Nucleares,
Apartado Postal 18-1027, México D.F. 11801, México,
* *e-mail: jorge@nuclear.inin.mx*

Recibido el 1 de mayo de 2006; aceptado el 1 de noviembre de 2006

We use the Newtonian limit of a general scalar-tensor theory around a background field to study astrophysical effects. The gravitational theory modifies the standard Newtonian potential by adding a Yukawa term to it, which is quantified by two theoretical parameters: λ, the lenghtscale of the gravitational interaction and its strength, α. Within this formalism we firstly present a numerical study on the formation of bars in isolated galaxies. We have found for positive α that the modified gravity destabilizes the galactic discs and leads to rapid bar formation in isolated galaxies. Values of λ in the range ≈ 8 – 14 kpc produce strongest bars in isolated models. Then, we extent this work by considering tidal effects due to interacting galaxies. We send two spirals to collide and study the bar properties of the remnant. We characterize the bar kinematical properties in terms of our parameters (λ, α).

Keywords: Bar formation; galaxy interaction; scalar-tensor theory.

Usamos el límite newtoniano de una teoría escalar-tensorial general alrededor de un campo del fondo para estudiar efectos astrofísicos. La teoría gravitacional modifica el potencial newtoniano estándar, agregandole un término de Yukawa, el cual se cuantifica por dos parámetros teóricos: λ, la escala de longitud de la interacción gravitacional y α, su intensidad. Dentro de este formalismo primero presentamos un estudio numérico de la formación de barras en galaxias aisladas. Encontramos que para α positiva la gravedad modificada desestabiliza a los discos galácticos y lleva a una rápida formación de la barra en galaxias aisladas. Valores de λ en el rango de ≈ 8 – 14 kpc producen barras más pronunciadas en los modelos de galaxias aisladas. Después, extendemos este trabajo al considerar efectos de marea debido a galaxias que interaccionan. Enviamos dos galaxias espirales a colisionar para estudiar las características de la barra del remanente formado. Caracterizamos las propiedades cinemáticas de la barra en términos de nuestros parámetros (λ, α).

Descriptores: Formación de la barra; interacción de galaxias; teoría escalar-tensorial.

PACS: 04.50.+h, 04.25.Nx; 98.10.+z; 98.62.Gq; 98.62.Js

1. Introduction

In recent years there have been some attempts to explain observed gravitational effects that imply the existence of dark matter (DM) and dark energy (DE). These effects go from galactic to cosmological scales and we still do not know the nature of DM and DE, or if they are related to each other, or even if DM is unique or there is a set of dark multi-components. One possibility is that scalar fields (SF) play a role in the modified dynamics. Particularly, SF are often applied in cosmology to accomplish the Universe's accelerated expansion, inferred from Supernovae Ia redshifts, CMB Doppler peaks measurements, large-scale structure surveys and cosmological simulations [1–8]. For a review of all these topics see for instance [9].

The way in which SF couple to gravity is also unknown, simply because there is a lack of a unique fundamental theory that explains the intricate relationship of matter and its gravitational background. One possibility is that SF are coupled non-minimally to gravity, at a Lagrangian footing, as it happens when string theories are compactified to four space-time dimensions [10]. The resulting effective theory is a scalar-tensor theory (STT) of gravitation, that can generically be described by arbitrary scalar functions, apart from the geometrical part [11, 12]. In the past we have studied different effects of this type of theories in cosmology [13–18], and more recently we have considered the Newtonian limit of STT and apply it to astrophysical phenomena. We have computed potential-density pairs for various halo density profiles [19] and axisymmetric systems [20]. It was found that rotation curves and parameters of the SF. On the other hand, in Ref. 21 we have computed the effect of SF on the transfer of angular momentum between protogalaxies. In the present work, we pursue to study bars in spiral galaxies. Observations of spiral galaxies indicate that the presence of a bar is a common feature [22]. Instabilities in isolated stellar and gaseous discs lead to bar formation; see [23] for pioneer studies and [24, 25] for a modern view. The bar formation in isolated models has been widely studied both analytically and numerically [26–33, e.g.,] and it is studied using the above STT formalism in the first part of this paper. In the second part, we consider in dynamical effects of non-isolated systems which are found in clusters of galaxies. In this sense, it has been suggested that the observed bar in many spirals is the result of the gravitational interaction between two or more nearby galaxies. For instance, [34] has found that during the collision of two galaxies and between the first and the second closest approaches, the disc takes a transient bar shape. The gravitational interaction between the two galaxies gives rise to perturbations in the orbits of the stars that results in the formation of the bar.

Bar formation in stellar discs depends upon various simultaneous effects. In the case of collisions, the 2D-simulations have shown that these factors are [35]: rotation curve shape, disc-halo mass ratio, perturbation force and geometry. Additionally, simulations suffer from numerical effects such as low spatial and temporal resolution, too few particles representing the system, and an approximate force model. These effects were studied by us in Refs. [25, 36], where it was shown that specific parameter choices may change bar properties. Once numerical effects are controlled, we may investigate all the other model parameters, which in our case are (λ, α).

In the present paper we study the formation of bars as a product of both instabilities of isolated galaxies and as a result of the collision of two spirals in framework of STT. In particular, we consider a non-minimally coupled SF in the Newtonian limit (Sec. 2) and use the resulting modified gravitation force in our 3D-simulations. In this way, all collisionless particles mutually interact with the modified gravitational force. Then, we investigate isolated galaxies (Sec. 3) and head-on and off-axis impacts of two disc galaxies and the properties of tidally formed bars (Sec. 4). We finally draw some conclusions (Sec. 5).

2. Scalar–tensor theory and its Newtonian limit

A typical STT is given by the following Lagrangian [11, 12]:

$$\mathcal{L}=\frac{\sqrt{-g}}{16\pi}\left[-\phi R+\frac{\omega(\phi)}{\phi}(\partial\phi)^2-V(\phi)\right]+\mathcal{L}_M(g_{\mu\nu}), \quad (1)$$

from which we get the gravity and SF equations. Here $g_{\mu\nu}$ is the metric, $\mathcal{L}_M(g_{\mu\nu})$ is the matter Lagrangian and $\omega(\phi)$ and $V(\phi)$ are arbitrary functions of the SF. Thus the gravitational equation is

$$R_{\mu\nu}-\frac{1}{2}g_{\mu\nu}R=\frac{1}{\phi}\left[8\pi T_{\mu\nu}+\frac{1}{2}Vg_{\mu\nu}+\frac{\omega}{\phi}\partial_\mu\phi\,\partial_\nu\phi -\frac{1}{2}\frac{\omega}{\phi}(\partial_\mu\phi)^2 g_{\mu\nu}+\phi_{;\mu\nu}-g_{\mu\nu}\Box\phi\right]. \quad (2)$$

The SF part is described by the following equation

$$\Box\phi+\frac{\phi V'-2V}{3+2\omega}=\frac{1}{3+2\omega}\left[8\pi T-\omega'(\partial\phi)^2\right], \quad (3)$$

where a prime (') denotes the derivative with respect to SF (ϕ).

In accordance with the Newtonian approximation, gravity and SF are weak. Then, we expect to have small deviations of the SF around the background field. Assuming also that the velocities of stars and DM particles are non-relativistic, we perform the expansion of the field equations around the background quantities $\langle\phi\rangle$ and $\eta_{\mu\nu}$. Even though the expansion of the above equations to first order is well known [37–39], we explicitly show it in the appendix since our definition of the background field is $\langle\phi\rangle=G_N^{-1}(1+\alpha)$, which is non-trivial, and this changes some constant terms in the equations. Accordingly, we obtain Eqs. (A.16) and (A.22):

$$\frac{1}{2}\nabla^2 h_{00}=\frac{G_N}{1+\alpha}\left[4\pi\rho-\frac{1}{2}\nabla^2\bar{\phi}\right], \quad (4)$$

$$\nabla^2\bar{\phi}-m^2\bar{\phi}=-8\pi\alpha\rho, \quad (5)$$

where ρ is matter density of DM or stars stemming from the energy-momentum tensor, G_N is the Newtonian gravitational constant and $\alpha\equiv 1/(3+2\omega)$ is a constant, in which ω is the Brans–Dicke parameter [11], here defined in theories that include scalar potentials. Equations (4) and (5) represent the Newtonian limit of a set of STT with arbitrary potentials ($V(\phi)$) and functions $\omega(\phi)$ that are Taylor expanded around some value. The resulting equations are thus distinguished by the constants α and m.

In the above expansion we have set the cosmological constant equal to zero since within galactic scales its influence is negligible. This is because the average density in a galaxy is much larger than a cosmological constant that is compatible with observations. Thus, we only consider the influence of luminous and dark matter. These matter components gravitate in accordance with the modified–Newtonian theory determined by Eqs. (4) and (5). The latter is a Klein-Gordon equation which contains an effective mass m term, whose Compton wavelength ($\lambda=h/mc$) implies a length scale for the modified dynamics. We shall assume this scale to be of the order of tens of kilo-parsecs, which corresponds to a very small mass, $m\sim 10^{-26}$ eV.

Note that Eq. (4) can be cast as a Poisson equation for $\psi\equiv(1/2)(h_{00}+\bar{\phi}/\langle\phi\rangle)$,

$$\nabla^2\psi=4\pi G_N\,\rho/(1+\alpha)\,, \quad (6)$$

Thus, the modified Newtonian potential is now given by

$$\Phi_N\equiv\frac{1}{2}h_{00}=\psi-\frac{1}{2}\frac{\bar{\phi}}{\langle\phi\rangle}\,. \quad (7)$$

Particular solutions, the so-called potential–density pairs [40], were recently found for the NFW's and Dehnen's density profiles [19] and for axisymmetric systems [20]. For point masses (of non-SF nature) the solution is well known [39, 41] and here is adapted to our definition of the background field, $\langle\phi\rangle=G_N^{-1}(1+\alpha)$:

$$\bar{\phi}=2\alpha u_\lambda\,, \quad \Phi_N=-u-\alpha u_\lambda\,, \quad (8)$$

where

$$u = \frac{G_N}{(1+\alpha)}\sum_s\frac{m_s}{|\mathbf{r}-\mathbf{r}_s|}\,, \quad (9)$$

$$u_\lambda = \frac{G_N}{(1+\alpha)}\sum_s\frac{m_s}{|\mathbf{r}-\mathbf{r}_s|}\mathrm{e}^{-|\mathbf{r}-\mathbf{r}_s|/\lambda}\,, \quad (10)$$

with m_s being a source mass. The potential u is the Newtonian part and u_λ is the SF modification which is of Yukawa type. The total gravitational force on a particle of mass m_i is

$$\mathbf{F}=-m_i\nabla\Phi_N=m_i\mathbf{a}. \quad (11)$$

Thus, gravitating particles, that in our simulations are stars or DM particles, will feel the influence of Newtonian gravity (u) plus a SF force due to the term u_λ.

The gravitational potential of a single particle arising from the above formalism is:

$$\Phi_N = \frac{G_N m_s}{(1+\alpha)\, r}(1+\alpha e^{-r/\lambda})\,, \qquad (12)$$

For local scales, $r \ll \lambda$, deviations from the Newtonian theory are exponentially suppressed, and for $r \gg \lambda$ the Newtonian constant diminishes (augments) to $G_N/(1+\alpha)$ for positive (negative) α. This means that equation (12) fulfills all local tests of the Newtonian dynamics, and it is only constrained by experiments or tests on scales larger than -or of the order of- λ, which in our case is of the order of galactic scales. By contrast, if one defines $\langle\phi\rangle \equiv 1/G_N$, then the effective Newtonian constant is modified at scales $r < \lambda$, and stringent, local constraints applies, demanding α to be less than 10^{-10} [41]. This latter approach will not be considered here.

Recently, the effect of STT has been investigated in different cosmological scenarios in which variations of the Newtonian constant are constrained from a phenomenological point of view. For instance, [42] studied the influence of varying G_N on the Doppler peaks of the CMBR, and concluded that their parameter ($\xi = G/G_N$) can be in the interval $0.75 \leq \xi \leq 1.74$ to be within the error bars of the CMBR measurements. In our notation this translates into $-0.43 \leq \alpha \leq 0.33$. However, this range for α has to be taken as a rough estimation, since these authors have only considered a variation of G_N, and not a full perturbation study within STT. The latter has been done by Ref. 43, who found some allowed deviations from the Newtonian dynamics, that translated into our parameter is $\alpha = 0.04$; however, a comparison with observations in not made. On the other hand, a structure formation analysis has been done in Ref. 44, in which deviations of the matter power spectrum are studied by adding a Yukawa potential to the Newtonian. They found some allowed dynamics, that turns out to constrain our parameter to be within $-1.0 \leq \alpha \leq 0.5$; but again a self-consistent perturbation study in general STT is missing. Thus, the above three estimates can be taken as order-of-magnitude constraints for our models. Note that even when it is not theoretically justified to take negative values for α, phenomenology admits them. In this work, however, we only consider positive values of α.

3. Isolated galaxy simulations

We use the standard procedure to construct a galaxy model with a Newtonian potential described in Refs. 25 and 36. The galaxy consists of a disc, halo, and bulge and its initial condition is constructed using the Hernquist halo model (a Dehnen's family member with $\gamma = 1$, see Ref. 19). To perform the 3D-simulations we used the *gbsph* code (www.astro.inin.mx/mar/nagbody) modified to include the contribution of the scalar fields as given in the preceding section. The forces were computed with a tolerance parameter $\theta = 0.75$, and including the quadruple term. We use Barnes's model parameters and system of units [24]. The mass, length and time scales are set to $2.2 \times 10^{11}\,\mathrm{M}_\odot = 1.40\,\mathrm{kpc} = 1$ and 250 Myr$= 1$, respectively. In these units, the gravitational constant is $G_N = 1$. The discs scale height is $z_0 = 0.007$ and the half mass radius of the galaxy is located at $R_{1/2} \approx 11$ kpc.

All isolated runs were performed with $\varepsilon = 0.015$ ($= 0.6$ kpc) and $\Delta t = 1/128$ for $N = 40\,960$, and $\varepsilon = 0.008$ and $\Delta t = 1/128$ for $N = 163\,840$, respectively. Galaxies were evolved up to $t = 12$ (3 Gyrs). Results of some of the runs are summarized in Table I, where columns are: the model label (1), the number of particles (2), the SF strength α (3), and SF length scale λ (4). As a result of simulations the following control parameters are displayed: the relative change of components of the disc velocity dispersions, measured at time 0.5 and 3 Gyrs (5-7) [36], the disc angular momentum loss (8), the Toomre's Q parameter (9), the Toomre's X parameter (10). The expressions for the last two parameters can be found in Ref. 40.

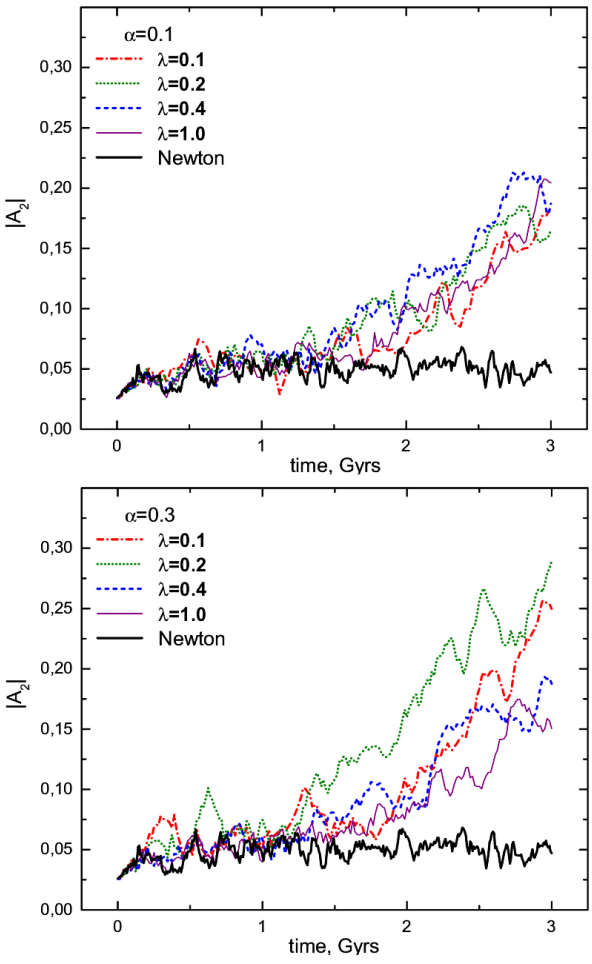

FIGURE 1. Evolution of $|A_2|$ for models SFB00-SFB04 (top panel) and for models SFC01-SFC04 (bottom panel).

TABLE I. Numerical parameters of galaxy evolution runs.

(1)	(2)	(3)	(4)	(5)	(6)	(7)	(8)	(9)	(10)
Model	N	α	λ	γ_r	γ_φ	γ_z	$\frac{\Delta L_{\rm d}}{L_{\rm d0}} \times 100$	Q	X_2
SFA00	40 960	0.0	-	0.724	0.734	1.037	4.1	2.5	2.2
SFA01	”	0.3	1.0	1.096	0.933	1.404	6.1	3.0	2.0
SFA02	”	0.3	0.4	1.051	0.936	1.262	4.5	2.8	2.0
SFA03	”	0.3	0.2	2.049	1.576	1.608	8.4	3.0	1.5
SFA04	”	0.3	0.1	1.673	1.345	1.114	7.7	2.9	1.0
SFB00	163 840	0.0	-	0.579	0.447	0.494	1.1	2.0	3.0
SFB01	”	0.1	1.0	0.898	0.687	0.636	2.7	2.5	3.0
SFB02	”	0.1	0.4	1.176	0.798	0.662	3.3	2.4	2.6
SFB03	”	0.1	0.2	1.058	0.805	0.617	2.9	2.3	2.5
SFB04	”	0.1	0.1	0.916	0.749	0.624	2.3	2.2	2.7
SFC01	”	0.3	1.0	0.889	0.653	0.593	4.4	2.5	2.5
SFC02	”	0.3	0.4	1.023	0.785	0.572	5.6	2.6	2.5
SFC03	”	0.3	0.2	1.779	1.325	0.764	8.8	3.0	1.7
SFC04	”	0.3	0.1	1.279	1.015	0.613	7.7	2.6	1.2

Table I shows, as in previous results [36], that experiments made with $N = 163\,840$ is less collisional than with smaller number of particles (compare columns 5–7). Runs series SFB are computed with SF strength $\alpha = 0.1$ and series SFC with $\alpha = 0.3$ and we observed that the heating of the disc is also higher for a higher SF strength.

In Fig. 1 we show the time evolution of the amplitude of the second harmonic, $|A_2|$, which tells us about the appearance of the bar at approximately 1.5 Gyr. The bar is stronger for $\alpha = 0.3$ than $\alpha = 0.1$, meanwhile in run SFB00 (Newtonian) a bar appears only at $t \approx 4$ Gyrs. Also, the disc in presence of SF heats stronger than in Newtonian case. This is due to a bar that appears in all simulations with SF.

As it can be seen, a stronger SF produce stronger bars for intermediate λ, reaching $|A_2| \approx 0.3$ for models SFC02 and SFC03. We think that the enhanced heating and transfer of the disc angular momentum in runs SFB02 and SFC03 is due to a stronger and larger bar which in turn depends on SF parameters. The bar angular velocities neither depend on λ nor α and have initially the value $\Omega_p \approx 6$, which after ~ 1 Gyrs decrease to $\Omega_p \approx 5.7$ in code units.

From Fig. 1 it is seen that SF with $\alpha = 0.3$ and $\lambda = 0.2$ produces the strongest bar. This is probably due to some resonance of disc particle orbits with the selected λ, which is roughly equal to the bar's length. The same result can be seen in Fig. 2, where the final density contours of discs are plotted.

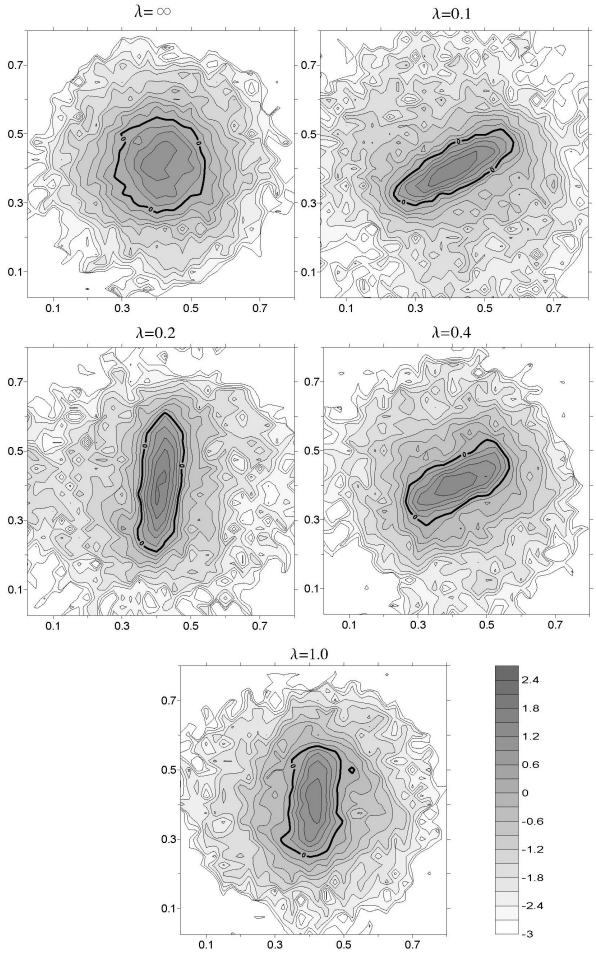

FIGURE 2. Projected disc density contours at $t = 3$Gyrs for models SFB00, SFC01-SFC04. Thick lines indicate zero level density contours in logarithmic scale.

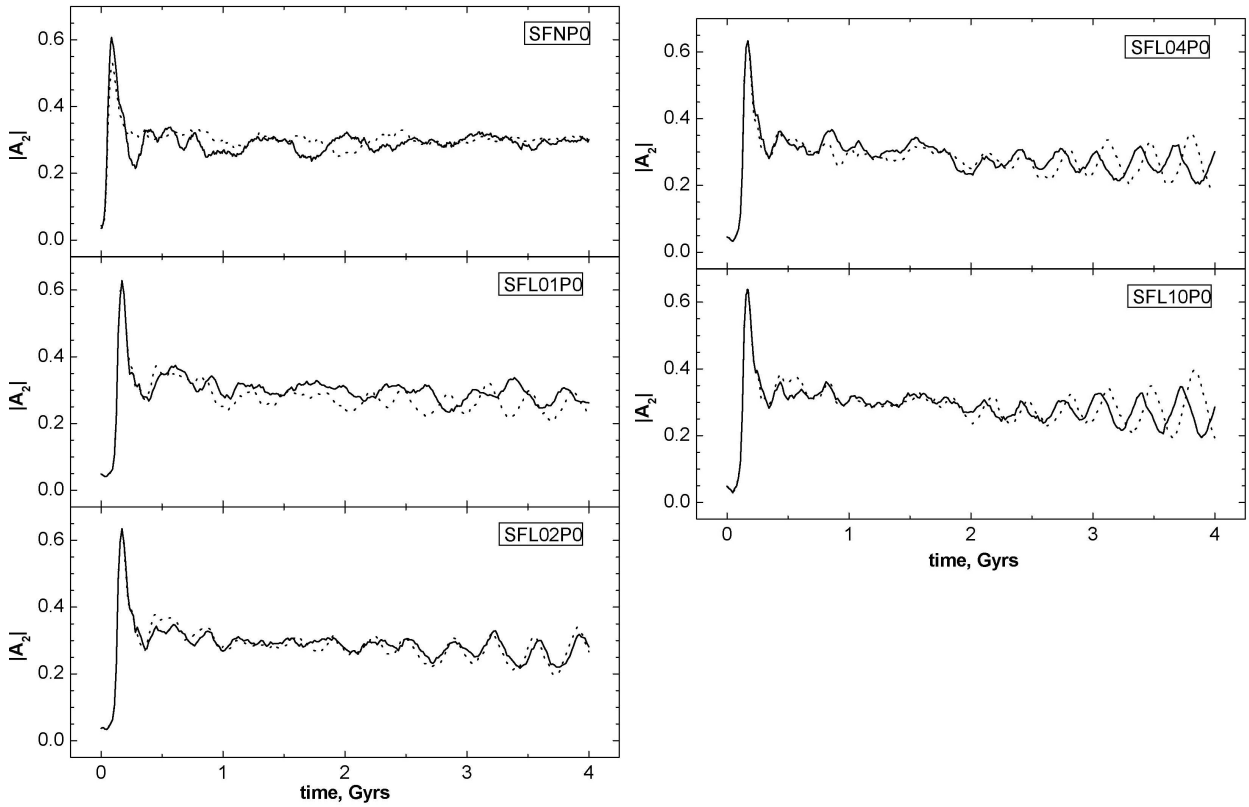

FIGURE 3. Evolution of $|A_2|$ for models SFNP0-SFL10P0. Dotted lines correspond to the first galaxy (retrograde orbit) whereas solid lines correspond to the second galaxy (prograde orbit).

4. Interacting galaxies simulations

In this section we describe 3D-simulations of collisions of two identical galaxies, each of which are the same as the used in study of isolated galaxies in the preceding section. In a recent paper [36] we have shown how the numerical parameters influence the bar properties. In accordance with this study we choose for the total number of particles $N = 163\,840$, the softening parameter $\varepsilon = 0.008$ and the time-step $\Delta t = 1/128$. This choice of parameters prevents from an early bar formation, hence, it permits to study the tidal effects on the bar formation.

We study the effect of the SF on tidal bar formation and its properties, such as its amplitude and rotational velocity. We compare the bar amplitude and its pattern speed for fixed α, varying λ and the impact parameter (p).

In order to maintain the same impact velocity and pericentric separation we have studied head-on and off-axis impacts of galaxies launched with the initial velocities $v = |v_x| = 200$ km/s and the impact parameter p, whose values are listed in Table I. The galaxies were relaxed up to $t = 0.25$ Gyrs before placed on the orbits with the initial separation $R = 64$ kpc. The whole collision is followed up to $t = 4$ Gyrs. We consider prograde-retrograde and planar collisions which allow us to investigate two possible directions of rotation and to check whether the bars emerge in retrograde discs during the violent collision. The first galaxy is retrograde, moves to the left and for off-axis collisions is placed above, whereas the second galaxy is prograde, moves to the right and is located below the first one.

TABLE II. Parameters of collisions with fixed $\alpha = 0.1$

Run	λ	p	Wiggle ? Disc 1	Wiggle ? Disc 2
SFL01P0	0.1	0	no	no
SFL01P1	-	0.4	yes	no
SFL01P2	-	0.8	yes	yes
SFL02P0	0.2	0	no	no
SFL02P1	-	0.4	yes	no
SFL02P2	-	0.8	yes	yes
SFL04P0	0.4	0	no	no
SFL04P1	-	0.4	yes	no
SFL04P2	-	0.8	yes	yes
SFL10P0	1.0	0	no	no
SFL10P1	-	0.4	yes	no
SFL10P2	-	0.8	no	yes
SFNP0	∞	0	no	no
SFNP1	-	0.4	yes	yes
SFNP2	-	0.8	no	yes

The performed collision simulations are summarized in Table II, where we have varied λ for a fixed value of the Yukawa strength $\alpha = 0.1$. We use the following labeling in model names: SF - for the scalar field, L(xx) - for the lambda value multiplied by ten, and P(y) - for the pericentric parameter expressed in number of disc radii. For the Newtonian simulations the SFN label is used. In all runs the total energy and the total angular momentum conserve better than 1%. Movies of some collision simulations are available at www.astro.inin.mx/ruslan/stt.

For all numerical experiments, we have plotted the evolution of the amplitude of the second harmonic, $|A_2|$, which indicates the presence of a bar and corresponding pattern velocity, Ω. We first consider head-on collisions. The graphics of $|A_2|$ and Ω shown in Figs. 3 and 4, respectively, are all similar and comparable to the Newtonian case, except for small oscillations at the end of the run. These oscillations increase with increasing λ and are also present in plots of bar pattern speed.

Next, we discuss simulations with an impact parameter equal to the disc's radius, $p = 16$ kpc. A striking difference between the run SFNP1 and runs SFL01P1-SFL10P1 is that for SF models the bars in both discs have roughly the same amplitude, independently of λ, whereas in Newtonian case their amplitudes differ by roughly twice, see Fig. 5. The fact that the retrograde discs form bars indicate that the discs in presence of SF are unstable and a short and strong enough perturbation is sufficient to produce a bar. As in Newtonian case, the retrograde bars are slightly faster than the prograde ones, indicating their similarity with isolated bars. In general, the pattern velocities of the prograde and retrograde bars for models with SF are smaller than for the Newtonian model, see Fig. 6.

Concerning encounters with $p = 32$ kpc, the curves in Figs. 7 and 8 are similar for each case and show no much difference. The only remarkable feature is the higher peaks in amplitudes of the prograde discs with SF in comparison with the Newtonian case.

In general, the presence of SF with positive α reduces the gravitation force on scales $r > \lambda$. In Ref. 36 we have seen that larger values of ε for the Plummer softening produce bars earlier. Thus, it is possible that the reduction of gravity either due to small ε or large λ is responsible for early formation of long bars. With negative α we expect to have a contrary result, *i.e.*, smaller bars that form later.

In addition, we have looked for morphological differences in spiral arms, such as the *wiggle* effect, which is the periodic change of the direction of short arms at the end of the bar from leading to trailing [36]. We visually search for the presence of the wiggle in both discs, and the results are listed in Table II.

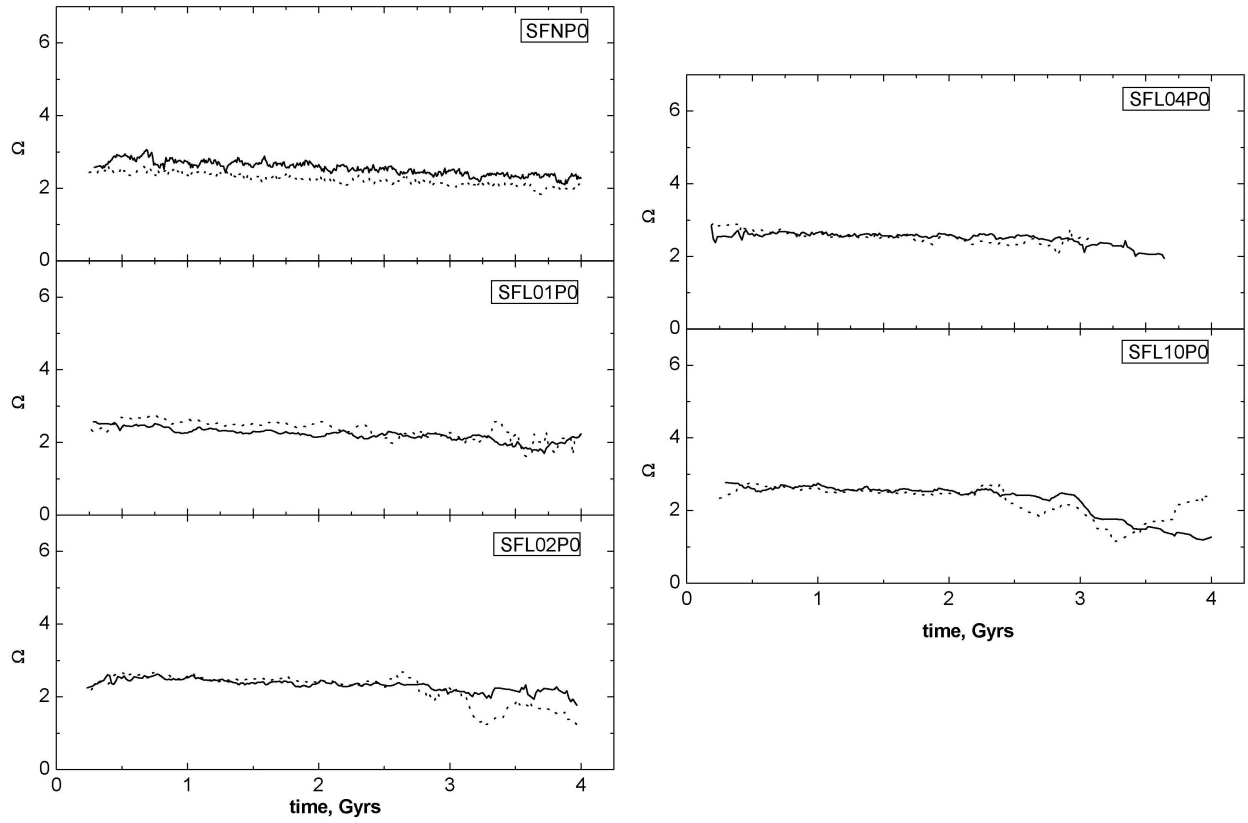

FIGURE 4. Evolution of Ω for models SFNP0-SFL10P0. The correspondence of curves is the same as in Fig. 3.

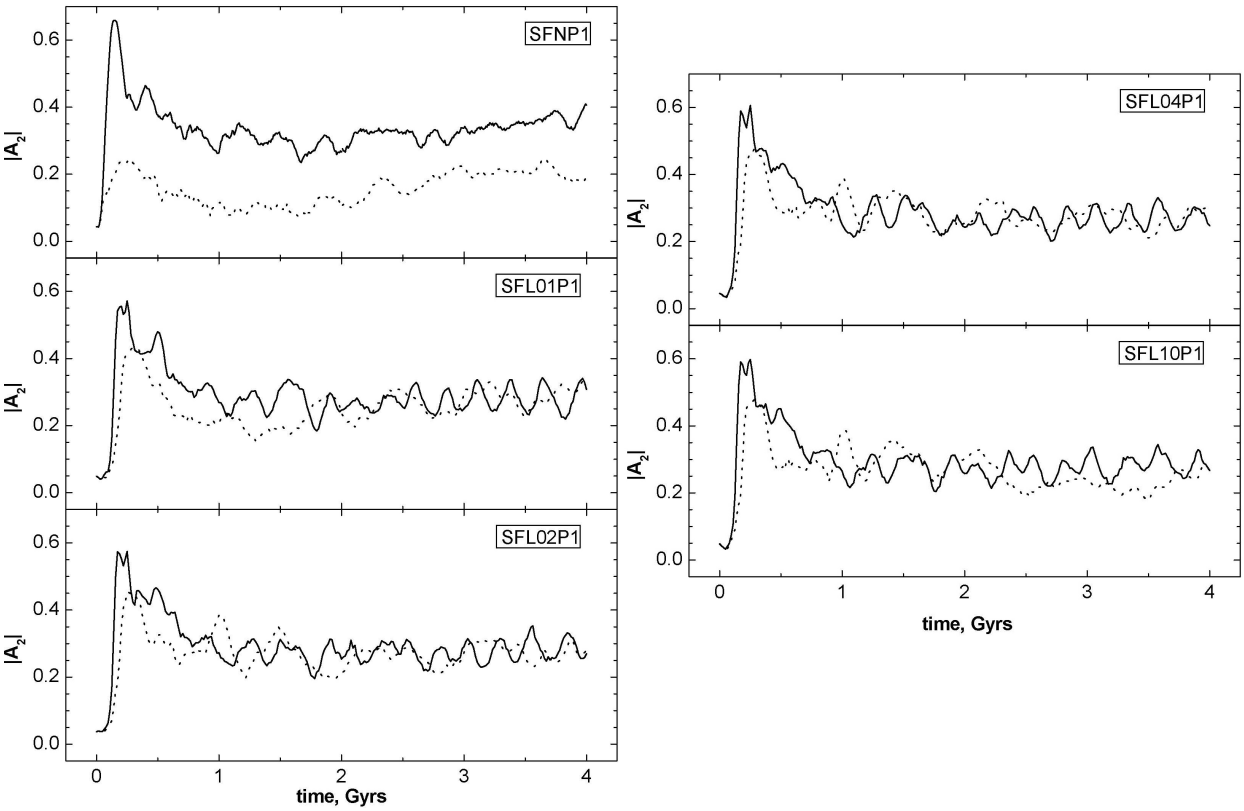

FIGURE 5. Evolution of $|A_2|$ for models SFNP1-SFL10P1. The correspondence of curves is the same as in Fig. 3.

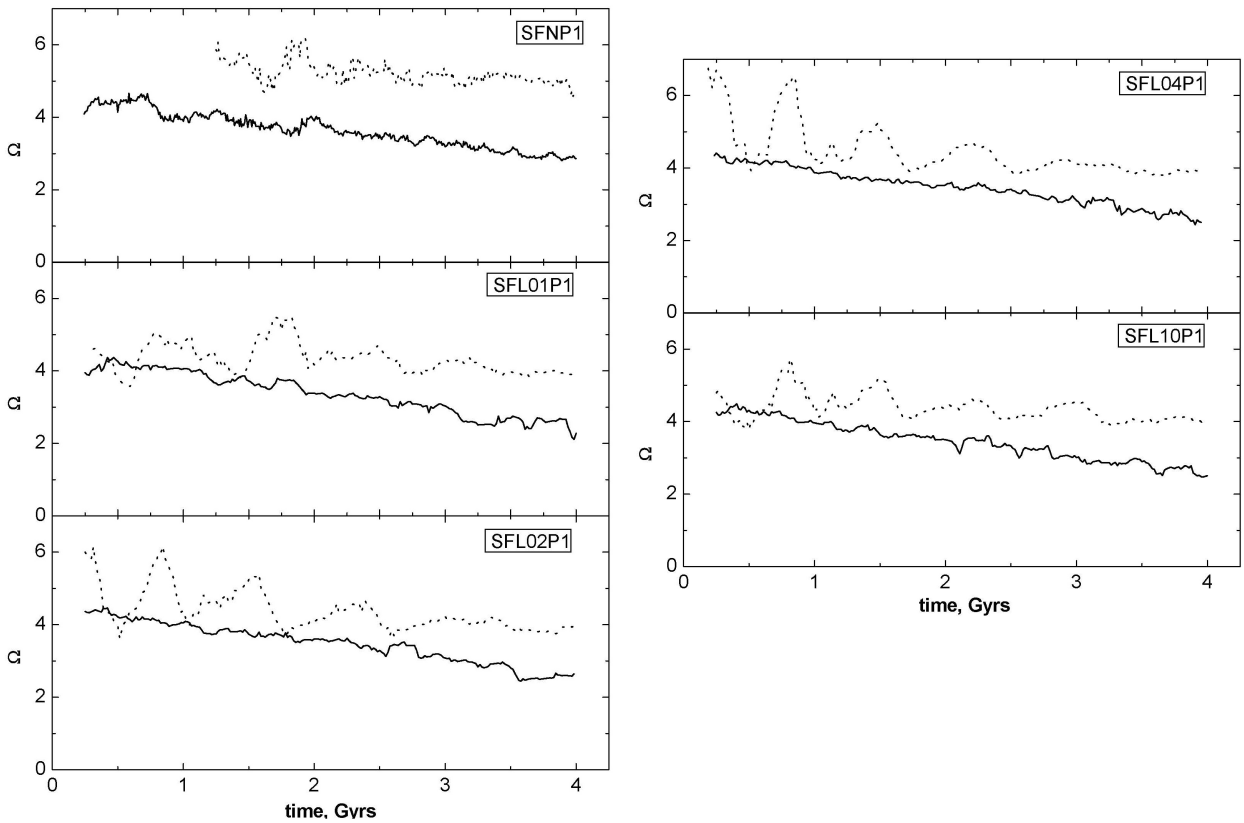

FIGURE 6. Evolution of Ω for models SFNP1-SFL10P1. The correspondence of curves is the same as in Fig. 3.

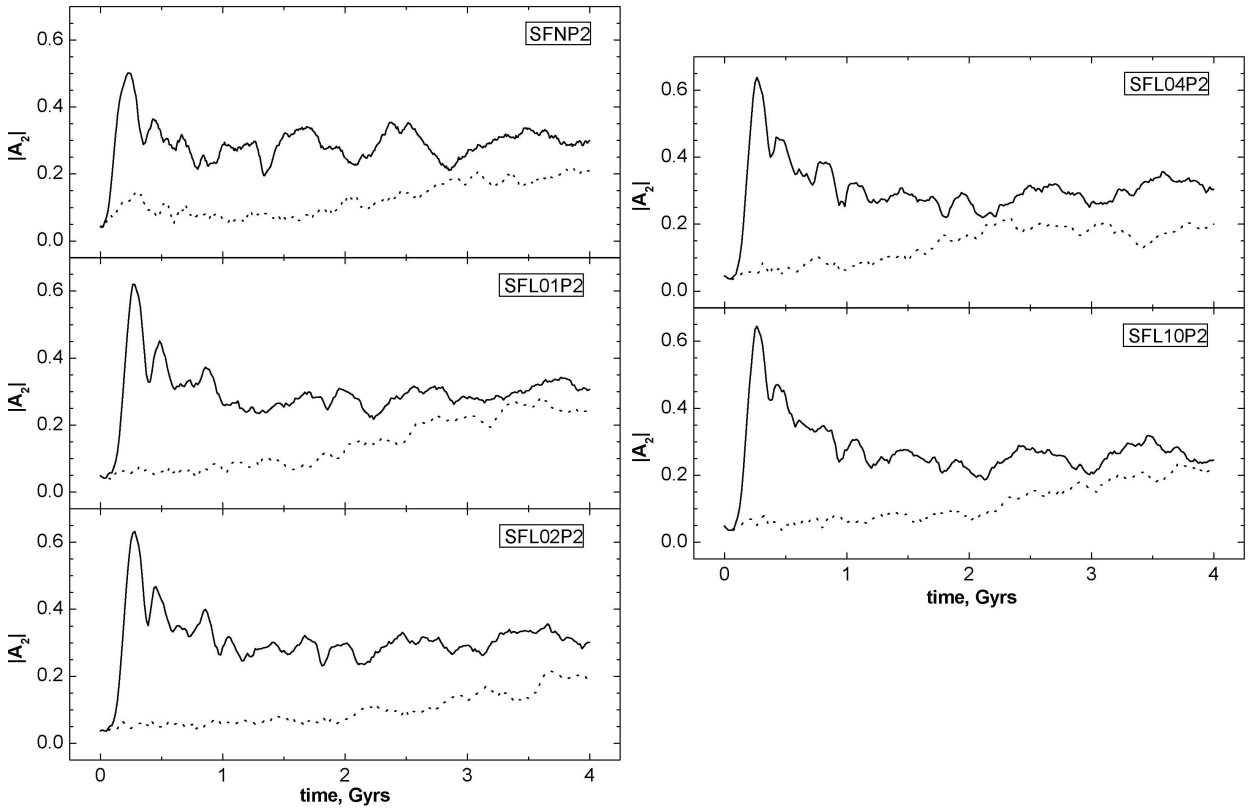

FIGURE 7. Evolution of $|A_2|$ for models SFNP2-SFL10P2. The correspondence of curves is the same as in Fig. 3.

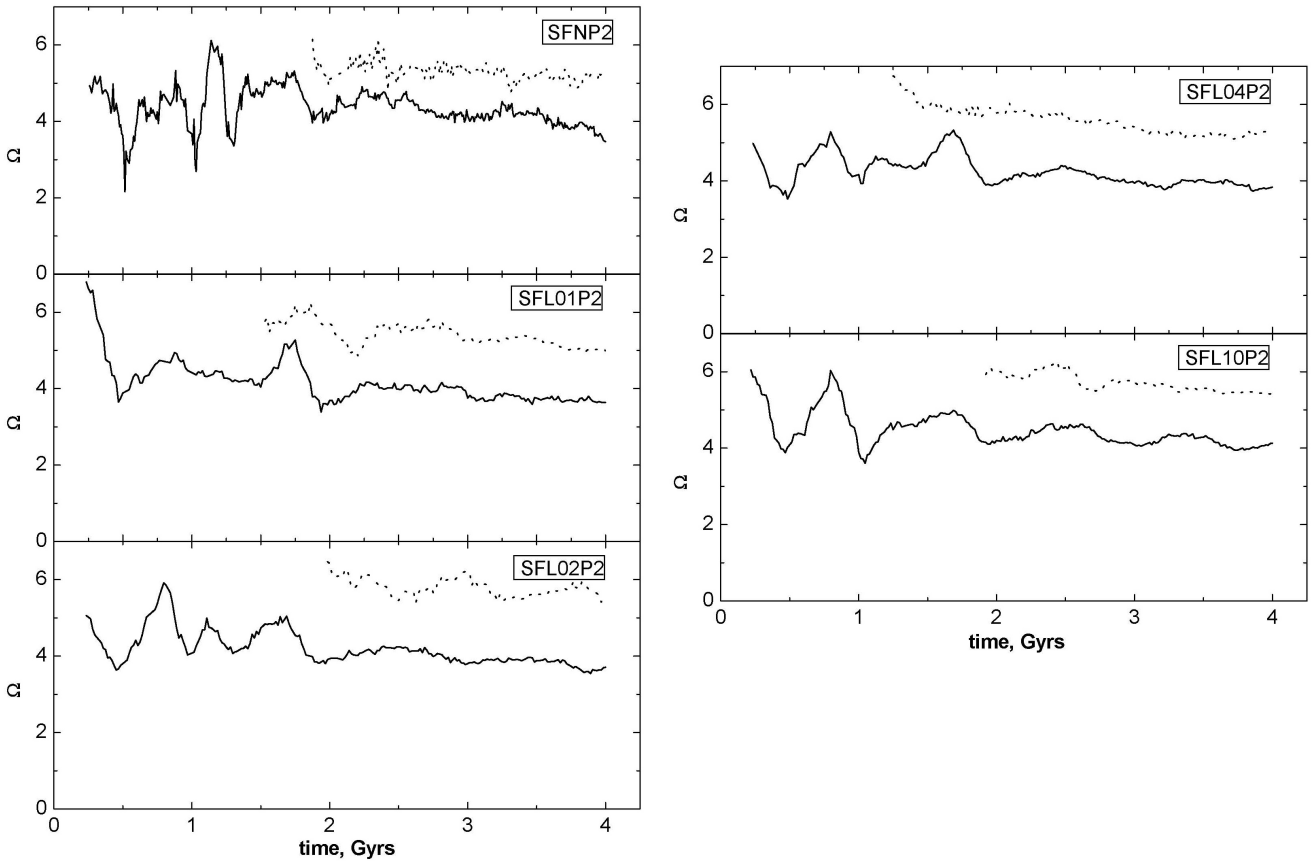

FIGURE 8. Evolution of Ω for models SFNP2-SFL10P2. The correspondence of curves is the same as in Fig. 3.

5. Conclusions

We have used the Newtonian limit of general STT that are compatible with local observations by the appropriate definition of the background field constant, *i.e.*, $\langle\phi\rangle = G_N/(1+\alpha)$. Then, from large-scale experiments we set a range of possible variations of the parameters of the modified gravitational theory, parametrized by (λ, α). The general gravitational effect is that the interaction with the SF becomes weaker ($\alpha > 0$) by a factor $1/(1+\alpha)$ for $r > \lambda$ in comparison with the Newtonian case. Using the resulting modified dynamics, we have studied isolated spirals and the collision of two equal spiral galaxies. From our simulations with different λ, we have found that the inclusion of the SF changes the dynamical properties of galaxies such as the bar morphology and pattern velocity.

From the performed simulations of isolated galaxy models with different λ, we can see that the addition of a non-minimally coupled SF slightly modifies the equilibrium of Newtonian model, acting as a perturbation, and diminishes the total potential energy, since the effective gravitational constant diminishes. This effect destabilizes the disc to form a bar in all models with $N = 163\,840$. For $\alpha = 0.1$, the SF interaction scale $\lambda = 16$ kpc produces a strongest bar, while for $\alpha = 0.3$, a strong bar forms for $\lambda = 8$ kpc. Also, for these scales bars appear earlier. This suggests that there exists some kind of resonance between stellar orbits and SF interaction scale. The results we have found with positive values of α imply that most of the spiral galaxies should be barred, but this does not exactly correspond with the observational fact that around 70% of isolated galaxies are barred [45]. However, the bar found might be the result of the algorithm to construct the initial models. Therefore, a next step is to construct a stable self-consistent model in accordance with the modified gravity. On the other hand, one could also study the effects for negative values of α, where the force augments for distances bigger than λ. A wide range of parameters should be investigated and higher resolution have to be used in simulations in order to make predictions for particular models.

In the study of isolated galaxies was shown that the presence of the SF destabilizes the disc of isolated galaxies and favors the bar formation. For collisions of two galaxies we observe the same trend. In the off-axis collisions with the impact parameter equal to the disc radius, the bars in both prograde and retrograde discs have the same amplitude, independently of λ. However, the wiggle does not appear in the second disc, as shown in Table II. All these properties depend on the pair (λ, α), which, on the other hand, can be constrained from observations that eventually will discriminate among the different values of the parameters of the theory.

The results presented are only preliminary, and we describe the overall differences without giving a full interpretation. A broad range of parameters should be investigated and higher resolution have to be used in simulations in order to make comparisons with the observed interacting galaxies.

Acknowledgements

This work has been partially supported by CONACYT under contracts U43534-R, 44917-F and J200.476/2004.

A The Newtonian limit of STT

We start with the field equations are given bye Eqs. (2) and (3) and compute the Newtonian limit of the scalar-tensor theory to first order. Accordingly, we assume that the potential oscillates around the background field

$$\phi = \langle\phi\rangle + \bar{\phi}, \qquad \langle\phi\rangle = \text{const.}\,, \tag{A.1}$$

and we expand the field quantities around $\langle\phi\rangle$ and the Minkowski metric ($g_{\mu\nu} = \eta_{\mu\nu} + h_{\mu\nu}$) to first order, being $\bar{\phi} \ll \langle\phi\rangle$ and $h_{\mu\nu} \ll \eta_{\mu\nu}$. We assume that the field is quasi-stationary, such that all time derivatives can be ignored: $\Box\phi = -\nabla^2\bar{\phi}$. Additionally, one has that $\rho c^2 \gg p$, and $T = T_{00} = \rho$.

With these assumptions we can expand all terms of field equations (2-3) and use Taylor series for the unknown functions $\omega(\phi)$ and $V(\phi)$ in terms of the small quantity $\bar{\phi}$. Let us first consider Eq. (2). The terms on the l.h.s., after inserting the perturbed metric and assuming the linearized harmonic gauge, can be written as:

$$R_{\mu\nu} - \frac{1}{2}g_{\mu\nu}R = \frac{1}{2}\left(h_{\mu\nu} - \frac{1}{2}\eta_{\mu\nu}h\right)^{,\lambda}_{\ \ ,\lambda}, \tag{A.2}$$

where $h = h^{\mu}_{\mu}$. The first term on the r.h.s. is the usual general relativity term. The second term can be written as follows:

$$\frac{1}{2}Vg_{\mu\nu} = \frac{1}{2}V\left(\eta_{\mu\nu} + h_{\mu\nu}\right). \tag{A.3}$$

The third and fourth terms vanish because these are second order terms in the expansion:

$$\partial_\mu\phi\partial_\nu\phi = \partial_\mu\bar{\phi}\partial_\nu\bar{\phi}. \tag{A.4}$$

The last two terms can be written as

$$\phi_{;\mu\nu} - g_{\mu\nu}\Box\phi = \bar{\phi}_{;\mu\nu} + \eta_{\mu\nu}\nabla^2\bar{\phi}, \tag{A.5}$$

and

$$\bar{\phi}_{;\mu\nu} = \left(\bar{\phi}_{,\mu}\right)_{;\nu} = \bar{\phi}_{,\mu\nu} - \Gamma^{\beta}_{\mu\nu}\bar{\phi}_{,\beta}. \tag{A.6}$$

Substituting the above expansions into Eq. (2) we may write:

$$\begin{aligned}\frac{1}{2}\left(h_{\mu\nu}-\frac{1}{2}\eta_{\mu\nu}h\right)^{,\lambda}_{\ \ ,\lambda} =& -\left[\frac{1}{\langle\phi\rangle}-\frac{1}{\langle\phi\rangle^2}\bar{\phi}\right]\\ &\times\left[8\pi T_{\mu\nu}-\frac{V}{2}\left(\eta_{\mu\nu}+h_{\mu\nu}\right)+\bar{\phi}_{;\mu\nu}\right.\\ &\left.+\left(\eta_{\mu\nu}+h_{\mu\nu}\right)\nabla^2\bar{\phi}\right]\end{aligned} \tag{A.7}$$

If we multiply the Eq. (A.7) by $\eta^{\mu\nu}$ and take the trace, the l.h.s. can be written as

$$\frac{1}{2}\left(\eta^{\mu\nu}h_{\mu\nu}-\frac{1}{2}\eta^{\mu\nu}\eta_{\mu\nu}h\right)^{,\lambda}_{\ ,\lambda} = \frac{1}{2}\left(h-2h\right)^{,\lambda}_{\ ,\lambda} = -\frac{1}{2}h^{,\lambda}_{\ ,\lambda}\,, \tag{A.8}$$

and the r.h.s. as

$$-\left[\frac{1}{\langle\phi\rangle}-\frac{1}{\langle\phi\rangle^2}\bar{\phi}\right] \times\left[8\pi\rho-\frac{V}{2}(4+h)-\nabla^2\bar{\phi}+(4+h)\nabla^2\bar{\phi}\right]. \tag{A.9}$$

In the last equation we used the relation

$$\bar{\phi}_{,\nu}{}^{,\nu}=-\nabla^2\bar{\phi}, \tag{A.10}$$

valid to first order. Now, let us rewrite the Eq. (A.2) as follows:

$$\frac{1}{2}\left(h_{\mu\nu}-\frac{1}{2}\eta_{\mu\nu}h\right)^{,\lambda}_{\ ,\lambda}=\frac{1}{2}\left(h^{,\lambda}_{\mu\nu,\lambda}-\frac{1}{2}\eta_{\mu\nu}h^{,\lambda}_{\ ,\lambda}\right), \tag{A.11}$$

in which we insert A.9 instead of the term $-h^{,\lambda}_{\ ,\lambda}$ and using Eq. (A.7) we obtain

$$\begin{aligned}&\frac{1}{2}h^{,\lambda}_{\mu\nu,\lambda}-\frac{1}{2}\eta_{\mu\nu}\left[\frac{1}{\langle\phi\rangle}-\frac{1}{\langle\phi\rangle^2}\bar{\phi}\right]\\ &\times\left[8\pi\rho-\frac{V}{2}(4+h)+h\nabla^2\bar{\phi}+3\nabla^2\bar{\phi}\right]\\ &=-\left[\frac{1}{\langle\phi\rangle}-\frac{1}{\langle\phi\rangle^2}\bar{\phi}\right]\left[8\pi T_{\mu\nu}-\frac{V}{2}\left(\eta_{\mu\nu}+h_{\mu\nu}\right)\right.\\ &\left.+\bar{\phi}_{;\mu\nu}+\left(\eta_{\mu\nu}+h_{\mu\nu}\right)\nabla^2\bar{\phi}\right].\end{aligned} \tag{A.12}$$

Let $\mu=\nu=0$. Then, the above equation becomes to first order

$$\begin{aligned}&\frac{1}{2}h^{,\lambda}_{00,\lambda}\equiv-\nabla^2\Phi\\ &=-\left[\frac{1}{\langle\phi\rangle}\right]\left[4\pi\rho+\frac{V}{2}-\frac{V}{2}h_{00}+\frac{Vh}{4}-\frac{1}{2}\nabla^2\bar{\phi}\right]\\ &+\left[\frac{\bar{\phi}}{\langle\phi\rangle^2}\right]\left[4\pi\rho+\frac{V}{2}\right],\end{aligned} \tag{A.13}$$

where Φ is modified Newtonian potential. Here we used the fact that

$$\frac{1}{2}\left(h_{00}\right)^{,\lambda}_{\ ,\lambda}=\frac{1}{2}\left(h_{00}\right)^{,0}_{\ ,0}-\frac{1}{2}\left(h_{00}\right)^{,i}_{\ ,i} =-\frac{1}{2}\left(h_{00}\right)^{,i}_{\ ,i}=\frac{1}{2}\nabla^2h_{00}. \tag{A.14}$$

Finally, expanding the potential

$$V=V(\langle\phi\rangle)+\left.\frac{\partial V}{\partial\bar{\phi}}\right|_{\langle\phi\rangle}\bar{\phi}+\cdots, \tag{A.15}$$

and discarding terms higher than first order we reach the the expression

$$\frac{1}{2}\nabla^2\Phi_N=\frac{1}{\langle\phi\rangle}\left[4\pi\rho-\frac{1}{2}\nabla^2\bar{\phi}\right]. \tag{A.16}$$

Accordingly, particles in our galactic models experience a force given by $\mathbf{F}=-\nabla\Phi_N$. Now, consider Eq. (3). The terms that depend on ϕ can be expanded to the first order:

$$\begin{aligned}\frac{1}{3+2\omega}&=\left.\frac{1}{3+2\omega}\right|_{(\langle\phi\rangle)}\\ &+\left.\frac{\partial}{\partial\bar{\phi}}\left(\frac{1}{3+2\omega}\right)\right|_{\langle\phi\rangle}\bar{\phi}+\cdots\end{aligned} \tag{A.17}$$

$$\omega'(\phi)=\omega'_{\langle\phi\rangle}+\omega''_{\langle\phi\rangle}\bar{\phi}+\cdots \tag{A.18}$$

Let us make the following notation:

$$V(\langle\phi\rangle)\equiv V_{\langle\phi\rangle},\quad \left.\frac{\partial V}{\partial\bar{\phi}}\right|_{\langle\phi\rangle}\equiv V'_{\langle\phi\rangle}. \tag{A.19}$$

$$\left.\frac{1}{3+2\omega}\right|_{(\langle\phi\rangle)}\equiv\alpha_{\langle\phi\rangle},\quad \left.\frac{\partial}{\partial\bar{\phi}}\left(\frac{1}{3+2\omega}\right)\right|_{\langle\phi\rangle}\equiv\alpha'_{\langle\phi\rangle}. \tag{A.20}$$

Substituting Eqs. (A.15), (A.17-A.20) into Eq. (3) and keeping only the terms up to the first order, we obtain:

$$\begin{aligned}&-\nabla^2\bar{\phi}+\alpha^2_{\langle\phi\rangle}\left[\alpha^{-1}_{\langle\phi\rangle}\left(\langle\phi\rangle V''_{\langle\phi\rangle}-V'_{\langle\phi\rangle}\right)\right.\\ &\left.-2\omega'_{\langle\phi\rangle}\left(\langle\phi\rangle V'_{\langle\phi\rangle}-2V_{\langle\phi\rangle}\right)+16\pi\rho\omega'_{\langle\phi\rangle}\right]\bar{\phi}\\ &=\alpha_{\langle\phi\rangle}\left[8\pi\rho+2V_{\langle\phi\rangle}-\langle\phi\rangle V'_{\langle\phi\rangle}\right].\end{aligned} \tag{A.21}$$

The constant in the second term of the l.h.s. represents an -squared- effective mass term of the theory that we will denote as m^2. Last two terms in the r.h.s. represent a cosmological constant that we will set to zero, since the mean density of the galaxy is much greater than this term. Accordingly, we finally have:

$$-\nabla^2\bar{\phi}+m^2\bar{\phi}=8\pi\alpha_{\langle\phi\rangle}\rho\,. \tag{A.22}$$

This equation together with Eq. (A.16) represent the Newtonian limit of general STT that can be expanded around the background quantities $\langle\phi\rangle$ and $\eta_{\mu\nu}$.

1. A.G. Riess *et al.*, *AJ.* **116** (1998) 1009.
2. S. Perlmutter *et al.*, *ApJ* **517** (1999) 565.
3. P. de Bernardis *et al.*, *Nat* **404** (2000) 995.
4. A.G. Riess *et al.*, *ApJ* **560** (2001) 49.
5. J.A. Peacock *et al*, 2002, to appear in "A New Era in Cosmology" (ASP Conference Proceedings), eds T. Shanks and N. Metcalfe, preprint (astro-ph/0204239).
6. G. Efstathiou, *MNRAS* **330** (2002) L29.
7. C.L. Bennett *et al.*, *ApJS* **148** (2003) 1.
8. Spergel *et al.* (2006), astro-ph/0603449.
9. N. Bretón, J.L. Cervantes-Cota, and M. Salgado (Eds.), 2004, *The Early Universe and Observational Cosmology*. Series: Lecture Notes in Physics, 646, Springer-Verlag, Heidelberg.
10. M.B. Green, J.H. Schwarz and E. Witten, Superstring Theory (Cambridge University Press, Cambridge 1988).
11. C. Brans and R. Dicke, *Phys. Rev. D* **124** (1961) 925.
12. R. Wagoner, *Phys. Rev. D* **1** (1970) 3209.
13. P. Chauvet, P. Cervantes-Cota and H.N. Núñez-Yépez, *Class. Quant. Grav.* **9** (1992) 1923.
14. J.L. Cervantes-Cota and H. Dehnen, *Phys. Rev. D* **51** (1995) 395.
15. J.L. Cervantes-Cota and H. Dehnen, *Nucl. Phys. B* **442** (1995) 391.
16. P Chauvet and J.L. Cervantes-Cota, *Phys. Rev. D* **52** (1995) 3416.
17. J.L. Cervantes-Cota and P. Chauvet, *Phys. Rev. D* **59** (1999) 043501-1.
18. J.L. Cervantes-Cota, *Class. and Quant. Grav*. **16** (1999) 3903.
19. M.A. Rodríguez-Meza and J.L. Cervantes-Cota, *MNRAS* **350** (2004) 671.
20. M.A. Rodríguez-Meza, J.L. Cervantes-Cota, M.I. Pedraza, J.F. Tlapanco and E.M. De la Calleja, *Gen. Rel. Grav.* **37** (2005) 823.
21. M.A. Rodríguez-Meza, J. Klapp, J.L. Cervantes-Cota, and H. Dehnen, in *Exact solutions and scalar fields in gravity: Recent developments*, Eds. Macias A., Cervantes-Cota J.L., and Lämmerzahl C. (Kluwer Academic/Plenum Publishers, NY, 2001) p. 213.
22. B.G. Elmegreen and D.M. Elmegreen, *ApJ* **267** (1983) 31.
23. A. Toomre, *ApJ* **139** (1964) 1217.
24. J.E. Barnes, in *Galaxies: Interaction and Induced Star Formation*, ed. D. Friedly, L.Martinet, and D.Pfenniger (Berlin: Springer-Verlag, 1998) p. 275.
25. R.F. Gabbasov, *Numerical simulation of bars in interacting galaxies*, Doctoral thesis, (Universidad Autónoma del Estado de México, Toluca. 2006).
26. F. Hohl, *ApJ* **168** (1971) 343.
27. J.A. Sellwood, *A&A* **99** (1981) 362.
28. J.A. Sellwood and R.G. Carlberg, *ApJ* **282** (1984) 61.
29. J.A. Sellwood and E. Athanassoula, *MNRAS* **221** (1986) 195.
30. E. Athanassoula and J.A. Sellwood, *MNRAS* **221** (1986) 213.
31. M.D. Weinberg, *MNRAS* **213** (1985) 451.
32. V.P. Debattista and J.A. Sellwood, *ApJ* **543** (2000) 704.
33. M.D. Weinberg and N. Katz, *ApJ* **580** (2002) 627.
34. M. Nogushi, *MNRAS* **228** (1987) 635.
35. H. Salo, *A&A* **243** (1990) 118.
36. R.F. Gabbasov, M.A. Rodríguez-Meza, J.L. Cervantes-Cota, and J. Klapp, *Astron. & Astrophys.* **449** (2006) 1043.
37. K. Nordtvedt Jr., *ApJ* **161** (1970) 1059.
38. C.M. Will, *Theory and experiment in gravitational physics*, Second. Ed. (Cambrigde University Press, 1992).
39. T. Helbig, *ApJ* **382** (1991) 223.
40. J. Binney and S. Tremaine, *Galactic Dynamics*, (Princeton Univ. Press, 1994).
41. E. Fishbach and C.L. Talmadge, *The Search for Non-Newtonian Gravity* (Springer-Verlag, NY, 1998).
42. K. Umezu, K.Ichiki, and M.Yahiro, *Phys.Rev. D* **72** (2005) 044010.
43. R. Nagata, T. Chiba, and N. Sugiyama, *Phys. Rev. D* **66** (2002) 103510.
44. A. Shirata, T. Shiromizu, N. Yoshida, and Y. Suto, *Phys. Rev. D* **71** (2005) 064030.
45. B.G. Elmegreen, D.M. Elmegreen, and A.C. Hirst, *ApJ* **612** (2004) 191.